



# Dynamic behaviors of mixed localized solutions for the three-component coupled Fokas–Lenells system

Minmin Wang · Yong Chen

Received: 17 August 2019 / Accepted: 1 October 2019 / Published online: 25 October 2019  
© Springer Nature B.V. 2019

**Abstract** We study the dynamic behaviors of mixed localized solutions for the three-component coupled Fokas–Lenells (FL) system. First, the corresponding Lax pair and the generalized  $(n, M)$ -fold Darboux transformation are constructed. Second, the first- and second-order mixed localized solutions of the three-component FL system are given and their dynamic features are investigated. These results further reveal the interesting dynamic behaviors of the higher-order mixed localized solutions in the multi-component coupled FL system. At last, the corresponding modulation instability is studied.

**Keywords** Darboux transformation · Mixed localized solutions · The three-component Fokas–Lenells system

## 1 Introduction

The Fokas–Lenells (FL) equation is a generalized form of the derivative Schrödinger equation, which was pro-

posed by Fokas [1] and Lenells and Fokas [2]. The soliton solutions of the FL equation describe the soliton dynamics in optical fibers [3]. Recently, a large and growing body of literature has investigated the soliton solution and the dynamic characteristic for the FL equation. By direct method, Matsuno [4] concluded the dark soliton solutions in 2012. Then Xu and Fan [5] investigated the long-time asymptotics with decaying initial value problem. Triki and Wazwaz [6] got some new types of chirped soliton solutions in 2017. Besides, the solitons, breathers and  $n$ -order rogue waves of FL equation were further studied by Darboux transformation (DT) [7,8]. Ahmed et al. [9] obtained M-shaped rational solitons and their interactions with kink waves. However, the mixed localized solutions for the three-component FL system have not been considered. Here we consider the following three-component FL system

$$\begin{aligned} u_{1,x} + \frac{i}{2}(2|u_1|^2 + \sigma|u_2|^2 + \sigma|u_3|^2)u_{1,x} \\ + \frac{i}{2}\sigma(u_2^*u_{2,x} + u_3^*u_{3,x})u_1 + u_1 = 0, \\ u_{2,x} + \frac{i}{2}(|u_1|^2 + 2\sigma|u_2|^2 + \sigma|u_3|^2)u_{2,x} \\ + \frac{i}{2}(u_1^*u_{1,x} + \sigma u_3^*u_{3,x})u_2 + u_2 = 0, \\ u_{3,x} + \frac{i}{2}(|u_1|^2 + \sigma|u_2|^2 + 2\sigma|u_3|^2)u_{3,x} \\ + \frac{i}{2}(u_1^*u_{1,x} + \sigma u_2^*u_{2,x})u_3 + u_3 = 0. \end{aligned} \quad (1)$$

---

The Project is supported by National Natural Science Foundation of China (Nos. 11675054, 11435005), Science and Technology Commission of Shanghai Municipality (No. 18dz2271000).

---

M. Wang · Y. Chen (✉)  
School of Mathematical Sciences, Shanghai Key  
Laboratory of PMMP, East China Normal University,  
Shanghai 200062, China  
e-mail: profchenyong@163.com

where  $u_k$  ( $k = 1, 2, 3$ ) is complex function for the independent variables  $x$  and  $t$ ,  $\sigma = \pm 1$  and the non-numeric subscripts variables in system (1) stand for the partial differentiation.  $u_k^*$  ( $k = 1, 2, 3$ ) denotes complex conjugate of  $u_k$  ( $k = 1, 2, 3$ ). In fact, in 2012, Kundu [10] derived a novel higher-order deformation of the FL equation, and system (1) is the generalized three-component form. Ling et al. [11] generalized the FL equation obtained in [10] to a two-component system, they constructed multi-bright soliton solution by generalized DT, and besides, they constructed multi-Hamiltonian structure and infinitely many conservation laws for the coupled FL system. Some typical rogue wave patterns such as the standard rogue wave, dark rogue wave and twisted rogue wave pair for the deformed FL equation were obtained in [12]. Xu and Chen [13] got some novel higher-order semi-rational solutions of the system in [11], which include higher-order rogue waves interacting with multi-bright or dark solitons, and higher-order rogue waves interacting with multi-breathers. However, for the corresponding three-component system, the various kinds of combination forms for the mixed localized solutions are more abundant and have not been investigated. In this present paper, we explore the dynamic behaviors of the mixed interaction solutions for the three-component coupled FL system (1) and the modulation instability.

Numerous studies were trying to get kinds of nonlinear waves for the nonlinear systems. Among them, solitons, breathers, rogue waves and their mixed forms arise from a balance of the nonlinearity and dispersion terms [14–16]. The rogue wave, whose amplitude is about three times than that of the plane wave and appear from nowhere and disappear from nowhere, was detected in [17]. Furthermore, the semi-rational solutions which perform as a mixed form of the breathers or solitons with rogue waves have been found in many integrable systems [18–24]. For the multi-component coupled system, the mixed localized solutions are more colorful than ones in the single-component nonlinear equations [25–30].

There are many efficient ways to get exact solutions of the nonlinear system, for example, the variable separation approach [31], the Hirota bilinear method [32–36], DT [37,38], Bäcklund transformation [39,40], Riemann–Hilbert method [41,42] and so on. Among them, DT is a momentous way to get new solutions of the nonlinear integrable system. A considerable amount of studies have been published on DT

[20–24,38,43]. By classical DT and take  $N$  different spectral parameters, the  $N$ -order solitons and  $N$ -order breathers can be obtained, but the same spectral parameter cannot be iterated twice. So based on the classical DT, Mateev derived the generalized DT [37]. By the generalized DT, many studies have investigated the higher-order rogue waves [20–22]. Successively, the semi-rational soliton solutions were researched widely [23,24,43]. Based on the above method, some meaningful results have been obtained. In order to get the mixed localized solutions of system (1), from the special vector solutions of Lax pair for system (1), we will explore the generalized  $(n, M)$ -fold DT of system (1). Then by dynamical analysis, some interesting dynamical features of the mixed localized solutions for system (1) will be exhibited.

The outline of this paper is organized as follows. In Sect. 2, we derive the Lax pair of the system (1), and the generalized  $(n, M)$ -fold DT of the system is constructed. In Sect. 3, we study the dynamic behaviors of the first- and second-order exact mixed localized solutions of system (1). Meanwhile, the dynamic behaviors of the mixed localized solutions for the multi-component FL system are exhibited. Section 4 investigates the modulation instability. Several conclusions and discussions are given in last section.

## 2 Lax pair and generalized $(n, M)$ -fold DT

In this section, we investigate the Lax integrability and construct the generalized  $(n, M)$ -fold DT of system (1).

### 2.1 Lax pair of system (1)

At first, the lax pair of system (1) is

$$\begin{aligned}\Phi_x &= U\Phi = \left(\frac{i}{\lambda^2}\sigma_3 + \frac{1}{\lambda}Qx\right)\Phi, \\ \Phi_t &= V\Phi = i\left(\frac{\lambda^2}{4}\sigma_3 - \frac{\lambda}{2}\sigma_3Q + \frac{1}{2}\sigma_3Q^2\right)\Phi,\end{aligned}\quad (2)$$

where

$$\begin{aligned}\sigma_3 &= \text{diag}(1, -1, -1, -1), \\ Q &= \begin{bmatrix} 0 & u_1^* & \sigma u_2^* & \sigma u_3^* \\ u_1 & 0 & 0 & 0 \\ u_2 & 0 & 0 & 0 \\ u_3 & 0 & 0 & 0 \end{bmatrix},\end{aligned}$$

$\Phi = (\phi_1, \phi_2, \phi_3, \phi_4)^T$  is a vector function,  $\lambda$  is the spectral parameter. In fact, it is easy to check that the

zero-curvature equation  $U_t - V_x + [U, V] = 0$  can directly lead to system (1).

### 2.2 The generalized $(n, M)$ -fold DT

The DT of the coupled two-component FL system has been constructed in [11, 13]. Based on the DT in [13] and the loop group method [19], we exhibit the following generalized  $(m, N)$ -fold DT of system (1).

Label  $\Phi_k$  as the solution of the linear spectral problem (2) when  $\lambda = \lambda_k$ . Derive the solution  $\Phi_{\lambda=\lambda'_k}$  of Lax pair when  $\lambda'_k = \lambda_k + \varepsilon$  ( $k = 1, 2, \dots, n$ ) by Taylor expansion at  $\varepsilon = 0$ .

$$\Phi_{\lambda=\lambda'_k} = \Phi_k^{[0]} + \Phi_k^{[1]}\varepsilon + \Phi_k^{[2]}\varepsilon^2 + \dots, \quad k = 1, 2, \dots, n, \tag{3}$$

where

$$\begin{aligned} \Phi_k^{[j]} &= \frac{1}{j!} \left. \frac{\partial^j \Phi_{\lambda=\lambda'_k}}{\partial \lambda_k^j} \right|_{\varepsilon=0} \\ &= (\phi_1[k, j], \phi_2[k, j], \phi_3[k, j], \phi_4[k, j])^T, \\ & \quad j = 1, 2, \dots, \end{aligned}$$

and  $k$  represents the spectrum parameter  $\lambda = \lambda_k$ ,  $j$  is corresponded with the coefficient of  $\varepsilon^j$ .

Then take advantage of a limit technique,

$$\begin{aligned} \Phi[k, j] &= \lim_{\varepsilon \rightarrow 0} \frac{(T[k, j-1] \dots T[k, 1] \Phi_{\lambda=\lambda'_k})_{\lambda=\lambda'_k}}{\varepsilon^j} \\ &= (\psi_1[k, j], \psi_2[k, j], \psi_3[k, j], \psi_4[k, j])^T, \end{aligned} \tag{4}$$

and construct the transformation

$$T[k, j] = \lambda^2 I + \Gamma_1[k, j] \lambda + \Gamma_0[k, j], \quad j=2, \dots, m_k, \tag{5}$$

where

$$\begin{aligned} \Gamma_1[k, j] &= (\lambda_k^{*2} - \lambda_k^2) N_1[k, j], \\ \Gamma_2[k, j] &= \lambda_1^* (\lambda_k^{*2} - \lambda_k^2) N_2[k, j] - \lambda_k^{*2} I, \\ N_1[k, j] &= \begin{bmatrix} \frac{|\psi_1[k, j]|^2}{\Delta[k, j]} & 0 \\ 0 & \frac{\mathbf{P}[k, j] \mathbf{P}[k, j]^\dagger}{\Delta^*[k, j]} \end{bmatrix}, \\ N_2[k, j] &= \begin{bmatrix} 0 & \frac{\phi_1[k, j] \mathbf{P}[k, j]^\dagger}{\Delta^*[k, j]} \\ \frac{\mathbf{P}[k, j] \phi_1^*[k, j]}{\Delta[k, j]} & 0 \end{bmatrix} \end{aligned}$$

with

$$\mathbf{P}[k, j] = (\psi_2[k, j], \psi_3[k, j], \psi_4[k, j])^T,$$

$$\begin{aligned} \Delta[k, j] &= \lambda_k |\psi_1[k, j]|^2 + \lambda_k^* (|\psi_2[k, j]|^2 \\ & \quad + |\psi_3[k, j]|^2 + |\psi_4[k, j]|^2). \end{aligned}$$

Take Eq. (5) as the solutions of the corresponding Lax pair system, we can formulate the generalized  $(n, M)$ -fold DT for system (1).

**Theorem 2.1** *Suppose  $\lambda_1, \lambda_2, \dots, \lambda_n$  are  $n$  different spectral parameters, then  $T_M = F_n F_{n-1} \dots F_1$  is a  $M$ -fold DT, where  $F_k = T[k, m_k] T[k, m_k - 1] \dots T[k, 1]$  with  $M = \sum_{k=1}^n m_k$ . Then*

$$u_k[M] = u_k[0] + \sum_{k=1}^n \sum_{j=1}^{m_k} \frac{(\lambda_k^{*2} - \lambda_k^2) \psi_1^*[k, j-1] \psi_k[k, j-1]}{D[j-1]}. \tag{6}$$

If  $n = M$ , the DT reduces to the elementary situation. By the reduced DT, we can obtain the  $N$  solitons and  $N$  breathers when begin with different background waves. If  $n = 1$ , the DT includes only one spectral parameter, which is similar to the DT in [11].

Begin with the nontrivial seed solution  $u_k[0] = c_k e^{i\theta}$  ( $k = 1, 2, 3$ ), where  $\theta = \frac{x}{\tau}$  and  $c_k$  is real constant. Then the vector eigenfunctions of the linear Lax system (2) can be denoted as  $\Phi = LMQ\Lambda$ , where

$$\begin{aligned} L &= \text{diag}(l_1, l_2, l_3, l_4), \\ M &= e^{\frac{1}{3}i\theta} \text{diag}(e^{-i\theta}, 1, 1, 1), \\ Q &= \begin{bmatrix} Q_{11} & Q_{12} & 0 & 0 \\ \lambda a_1 & \lambda a_1 & -\sigma a_2 & -\sigma a_3 \\ \lambda a_2 & \lambda a_2 & a_1 & 0 \\ \lambda a_3 & \lambda a_3 & 0 & a_1 \end{bmatrix}, \\ \Lambda &= \text{diag}(e^{\xi_1}, e^{\xi_2}, e^{\xi_3}, e^{\xi_3}) \end{aligned}$$

with

$$\begin{aligned} Q_{11} &= \frac{1}{2} \lambda^2 + \tau + \frac{1}{2} \sqrt{\lambda^4 + 4\tau^2}, \\ Q_{12} &= \frac{1}{2} \lambda^2 - \tau + \frac{1}{2} \sqrt{\lambda^4 + 4\tau^2}, \\ \xi_1 &= \frac{1}{6} \frac{(i\lambda^2 + 3i\sqrt{\lambda^4 + 4\tau^2})}{\lambda^2 \tau} x + \frac{i}{4} \sqrt{\lambda^4 + 4\tau^2} t, \\ \xi_2 &= \frac{1}{6} \frac{(i\lambda^2 - 3i\sqrt{\lambda^4 + 4\tau^2})}{\lambda^2 \tau} x - \frac{i}{4} \sqrt{\lambda^4 + 4\tau^2} t, \\ \xi_3 &= \frac{-i(\lambda^2 + \tau)}{\lambda^2 \tau} x - \frac{i}{4} \lambda^2 t \end{aligned} \tag{7}$$

and  $l_k$  is an arbitrary constant for  $k = 1, 2, 3, 4$ .

In order to get the semi-rational solutions of system (1), we set  $l_k$  appropriate value. Then  $\Phi$  can be rewritten as

$$\Phi = \begin{bmatrix} \phi_1 \\ \phi_2 \\ \phi_3 \\ \phi_4 \end{bmatrix} = \begin{bmatrix} (h_1 e^{\eta_1} - h_2 e^{-\eta_1}) e^{\eta_2} \\ \rho_1 (h_2 e^{\eta_1} - h_1 e^{-\eta_1}) e^{-\eta_2} - (\alpha a_2 \sigma + \beta a_3 \sigma) e^{\theta_0} \\ \rho_2 (h_2 e^{\eta_1} - h_1 e^{-\eta_1}) e^{-\eta_2} + a_1 \alpha e^{\theta_0} \\ \rho_3 (h_2 e^{\eta_1} - h_1 e^{-\eta_1}) e^{-\eta_2} + a_1 \beta e^{\theta_0} \end{bmatrix}, \tag{8}$$

where

$$\begin{aligned} \rho_1 &= \frac{a_1}{\sqrt{\tau}}, & \rho_2 &= \frac{a_2}{\sqrt{\tau}}, & \rho_3 &= \frac{a_3}{\sqrt{\tau}}, \\ \theta_0 &= \frac{-i(\lambda^4 t + 4x)}{4\lambda^2}, \\ \eta_1 &= \frac{i(\tau\lambda^2 + 2x)\sqrt{\lambda^4 + 4\tau^2}}{4\lambda^2\tau}, & \eta_2 &= \frac{-i}{2\tau}x, \\ h_1 &= \frac{\sqrt{\lambda^2 + 2\tau + \sqrt{\lambda^4 + 4\tau^2}}}{\sqrt{\lambda^4 + 4\tau^2}}, \\ h_2 &= \frac{\sqrt{\lambda^2 + 2\tau - \sqrt{\lambda^4 + 4\tau^2}}}{\sqrt{\lambda^4 + 4\tau^2}}. \end{aligned}$$

### 3 Dynamic behaviors of mixed localized solutions

Compared to the solutions of deformed FL system [10] and the two-component coupled FL system in [11, 13], the mixed localized solutions of the three-component system are more rich and varied. In this section, we analyze the dynamic behaviors of the first- and second-order mixed localized solutions. In the rest part of this paper, we take  $\sigma = 1$ .

#### 3.1 First-order mixed localized solutions

When  $n = 1$ , by the generalized  $(n, M)$ -fold DT in Theorem 3.1 and take the special vector solutions (8) of the Lax equation (2), then the first-order semi-rational solutions can be obtained as

$$\begin{aligned} u_1[1] &= a_1 e^{\frac{ix}{\tau}} \\ &+ \frac{-(\alpha a_2 + \beta a_3) \kappa_1 e^{\frac{i\tau^2 - (1-i)x}{2\tau}} + a_1 \kappa_2 e^{\frac{ix}{\tau}}}{\iota_1 e^{\frac{i\tau^2 - x}{\tau}} + \iota_2}, \\ u_2[1] &= a_2 e^{\frac{ix}{\tau}} \end{aligned}$$

$$\begin{aligned} &+ \frac{a_1 \alpha \kappa_1 e^{\frac{i\tau^2 - (1-i)x}{2\tau}} + a_2 \kappa_2 e^{\frac{ix}{\tau}}}{\iota_1 e^{\frac{i\tau^2 - x}{\tau}} + \iota_2}, \\ u_3[1] &= a_3 e^{\frac{ix}{\tau}} \\ &+ \frac{a_1 \beta \kappa_1 e^{\frac{i\tau^2 - (1-i)x}{2\tau}} + a_3 \kappa_2 e^{\frac{ix}{\tau}}}{\iota_1 e^{\frac{i\tau^2 - x}{\tau}} + \iota_2}, \end{aligned} \tag{9}$$

where  $\kappa_1, \kappa_2$  and  $\iota_2$  are complex functions in terms of  $(x, t)$ ,  $\iota_1$  is a polynomial of  $a_k (k = 1, 2, 3)$  and  $\alpha, \beta$

$$\begin{aligned} \kappa_1 &= 2\sqrt{2}\sqrt{1+i}i \left[ 2t\tau^4 + (-1+i)\tau^3 + 2ix\tau^2 \right], \\ \kappa_2 &= -(1+i)i \left[ (2t\tau^2 + i\tau)^2 - (2ix - \tau)^2 \right], \\ \iota_1 &= 2\sqrt{2}i\tau^3 \left[ (\alpha^2 + \beta^2)a_1^2 + (\alpha a_2 + \beta a_3)^2 \right], \\ \iota_2 &= (1+i) \left( 2x^2 - 2ix\tau + 2t^2\tau^4 \right. \\ &\quad \left. + 2i\tau^3t + \tau^2 \right). \end{aligned} \tag{10}$$

Equation (9) is three semi-rational complex functions which are consisted by the rational functions and exponential functions. We analyze the dynamic behaviors of these semi-rational solutions with different hybrid forms of rogue waves emerging during the propagation of various combination of breathers and solitons.

If  $\alpha = \beta = 0$ , then  $\iota_1 = 0$ , all of the three components reduced to a totally rational functions of  $(x, t)$ , which behave as the rogue waves with two peaks and two hollows. The plots of the rogue waves are similar to which in [44, 45], we omit them here.

#### Case 1.1. One-line bright or dark soliton with first-order rogue waves.

If some of the background waves are vanished and take some suitable parameter values, one component is one-line bright soliton with first-order rogue wave and the others are one-line dark solitons with first-order rogue waves. Another case is one one-line dark soliton with first-order rogue wave and two one-line bright solitons with first-order rogue waves.

- (1) Three different arrangements of two dark solitons with rogue waves and one bright soliton with rogue wave can be obtained. The first background wave is vanished ( $a_1 = 0$ ), and the others are non-vanished. Then, the first component  $u_1$  is a bright soliton with a weak first-order rogue-like wave and the others  $u_2, u_3$  are dark solitons with first-order rogue waves in Fig. 1a. If  $a_3 = 0$  and  $\alpha = 0$ ,

the first two components  $u_1, u_2$  are dark solitons with rogue waves and the third component  $u_3$  is a bright soliton with a weak rogue-like wave. Similar to the former situation, if  $a_2 = 0$  and  $\beta = 0$ , the components  $u_1, u_3$  transform to dark solitons with rogue waves and the component  $u_2$  is a bright soliton with a weak rogue-like wave.

- (2) If the second and third background waves are all vanished ( $a_2 = a_3 = 0$ ) and the first one is non-vanished ( $a_1 \neq 0$ ), the first component  $u_1$  is a dark soliton with a rogue wave and the other two component  $u_2, u_3$  are bright solitons with rogue-like waves (Fig. 1b).

Particularly, in Fig. 1, the rogue waves appearing in the propagation of the bright solitons are very weak. In fact, we even cannot call them rogue waves, because the altitude of the rogue waves is very low and the energy is very small compare to the propagating bright solitons. In other words, if the propagating waves perform as the bright solitons, the influence of the rogue waves which appear in the vicinity of  $t = 0$  is very weak.

**Case 1.2. One-line soliton or breather with first-order rogue waves.**

If only one of the parameters  $\alpha, \beta, a_2, a_3$  is zero, one of the components presents as a one-line bright or dark soliton with first-order rogue wave and the other two components are breathers with first-order rogue waves.

and  $\beta \neq 0$ , the second component  $u_2$  is a dark soliton with a rogue wave, but the other two components  $u_1$  and  $u_3$  are breathers with rogue waves. And the energy of the breathers in  $u_1$  and  $u_3$  also behaves opposite which is similar to that in Fig. 2b. If  $\alpha \neq 0$  and  $\beta = 0$ , the third component  $u_3$  is a dark soliton with rogue wave and the other two components  $u_1$  and  $u_2$  are breathers with rogue waves, we omit the corresponding plots here.

**Case 1.3. Breathers with first-order rogue waves.**

If  $a_k$  ( $k = 1, 2, 3$ ) and  $\alpha, \beta$  are all nonzero, three components  $u_k$  ( $k = 1, 2, 3$ ) are all present as the first-order rogue waves emerging in the propagation of breathers in Fig. 3. When  $\alpha = \beta = 10^{-4}$ , the rogue wave is separated with the breather in Fig. 3a, keep  $a_k$  ( $k = 1, 2, 3$ ) still and when  $\alpha = \beta$  increase to  $10^{-1}$ , the rogue waves stick together with the propagating breathers in Fig. 3b.

3.2 Second-order mixed localized solutions

In this section, we investigate the dynamic behaviors of the second-order mixed localized solutions for the system (1). Rewrite  $T[1, 2]_{\lambda=\lambda'}$  as  $(\lambda_1 + \varepsilon)^2 I + \Gamma_1[1, 2](\lambda_1 + \varepsilon) + \Gamma_0[1, 2]$  and substitute Eq. (3) into the limit below

$$\lim_{\varepsilon \rightarrow 0} \frac{T[1, 2]_{\lambda=\lambda'} \Phi_{\lambda=\lambda'}}{\varepsilon} = \lim_{\varepsilon \rightarrow 0} \frac{[(\lambda_1 + \varepsilon)^2 I + \Gamma_1[1, 2](\lambda_1 + \varepsilon) + \Gamma_0[1, 2]] [\Phi_1^{[0]} + \Phi_1^{[1]}\varepsilon + o(\varepsilon^2)]}{\varepsilon} = T[1, 2]\Phi_1^{[1]} + (2\lambda_1 I + \Gamma_1[1, 2]) \Phi_1^{[0]} = \Psi_1[2]. \tag{11}$$

- (1) If  $a_2 = 0$  or  $a_3 = 0$ , the second or third component is a bright soliton with rogue wave and the rest two components are breathers with rogue waves. When the third component  $u_3$  is the zero-plane ( $a_3 = 0$ ),  $u_3$  is a one-line bright soliton with a very weak rogue-like wave in Fig. 2a. The breathers in  $u_1$  and  $u_2$  are different. The energy and altitude for the upper half of the background plane  $u_1$  are much less than that for the lower half. But the breather in  $u_2$  performs as opposite dynamic features compares to  $u_1$ .
- (2) If  $\alpha = 0$  or  $\beta = 0$ , one component is a dark soliton with rogue wave and the rest two components are breathers with rogue waves. In Fig. 2b, set  $\alpha = 0$

Take the limit  $\Psi_1[2] = (\psi_1[2], \psi_2[2], \psi_3[2], \psi_4[2])^T$  as the new solution of the Lax pair (2). Then implementing the iterative formula (6) on the first-order solutions (9), we can get the second-order semi-rational solution  $u_k[2]$  where  $k = 1, 2, 3$ . The expression of  $u_k[2]$  is so cumbersome that we only show the iterative formula

$$u_k[2] = u_k[1] + \frac{(\lambda_1^2 - \lambda_1^{*2})\psi_1^*[2]\psi_k[2]}{D[2]}, \tag{12}$$

$k = 1, 2, 3,$

with  $D[2] = \lambda_1|\psi_1[2]|^2 + \lambda_1^*(|\psi_2[2]|^2 + |\psi_3[2]|^2 + |\psi_4[2]|^2)$ .

Here  $u_k[2]$  is a complex function of  $(x, t)$  with parameters  $a_k$  ( $k = 1, 2, 3$ ),  $\alpha, \beta$  and  $s = s_1 + is_2$ . Here

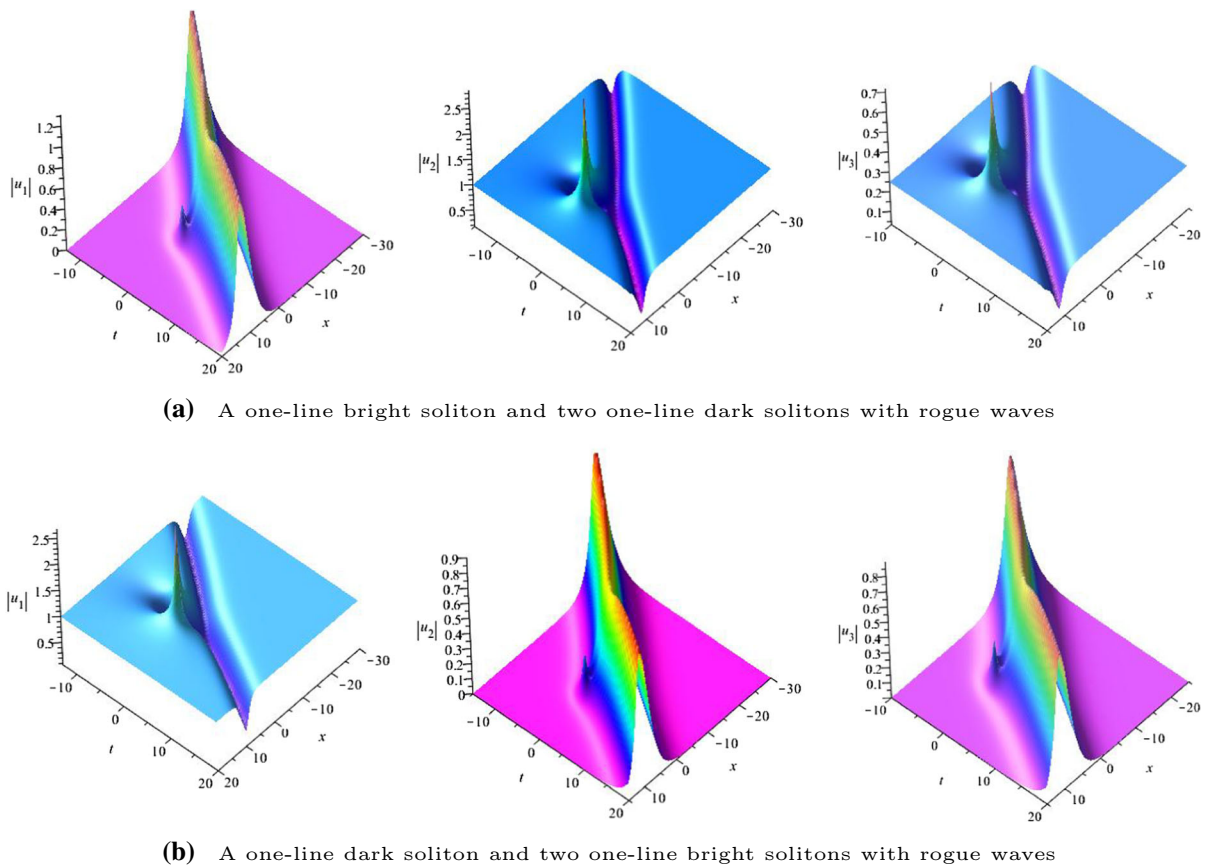


**Fig. 1** The 3-D map for case 1.1. Parameters with **a**  $a_1 = 0, a_2 = 1, a_3 = \frac{1}{4}, \alpha = \frac{1}{10}, \beta = \frac{1}{10}$ , **b**  $a_1 = 1, a_2 = 0, a_3 = 0, \alpha = \beta = \frac{1}{10}$  (Color online)

$s_1, s_2$  are arbitrary parameters to control the structures of higher-order rogue waves. Firstly, if  $\alpha = \beta = 0$ , the second-order rogue wave can be obtained in Fig. 4. When  $s_1 = s_2 = 10^3$ , one can get separated forms of the second-order rogue wave with the triangle patterns in the second line of Fig. 4.

Then similar to the analysis of the first-order solutions, we give three kinds of second-order mixed localized solutions of system (1).

### Case 2.1. Two-line bright or dark solitons with second-order rogue waves.

Similar to case 1.1, two different arrangements of with three two-line bright or dark solitons with second-order rogue waves can be obtained.

- (1) If the first background is vanished ( $a_1 = 0$ ) and  $a_2, a_3, \alpha, \beta \neq 0$ , in Fig. 5a, the first component  $u_1$  is a two-line bright soliton with second-order rogue-like wave, the second-order rogue-like wave

in  $u_1$  is much lower than the bright soliton. The other two components  $u_2, u_3$  are two-line dark solitons with second-order rogue waves.

- (2) If the second and third background waves are all vanished ( $a_2 = a_3 = 0$ ) and  $a_1, \alpha, \beta \neq 0$ , the first component  $u_1$  is a two-line dark soliton with the second-order rogue wave, and the other two components  $u_2, u_3$  are two-line bright solitons with the second-order rogue-like waves in Fig. 5b. The altitudes of the rogue-like waves in  $u_2, u_3$  are also very low and tend to zero. These results are consisted with that in the first-order case.

### Case 2.2. Two-line solitons or breathers with second-order rogue waves.

Under this case, one component is a two-line bright or dark soliton with second-order rogue wave and the other two are breathers with second-order rogue waves.

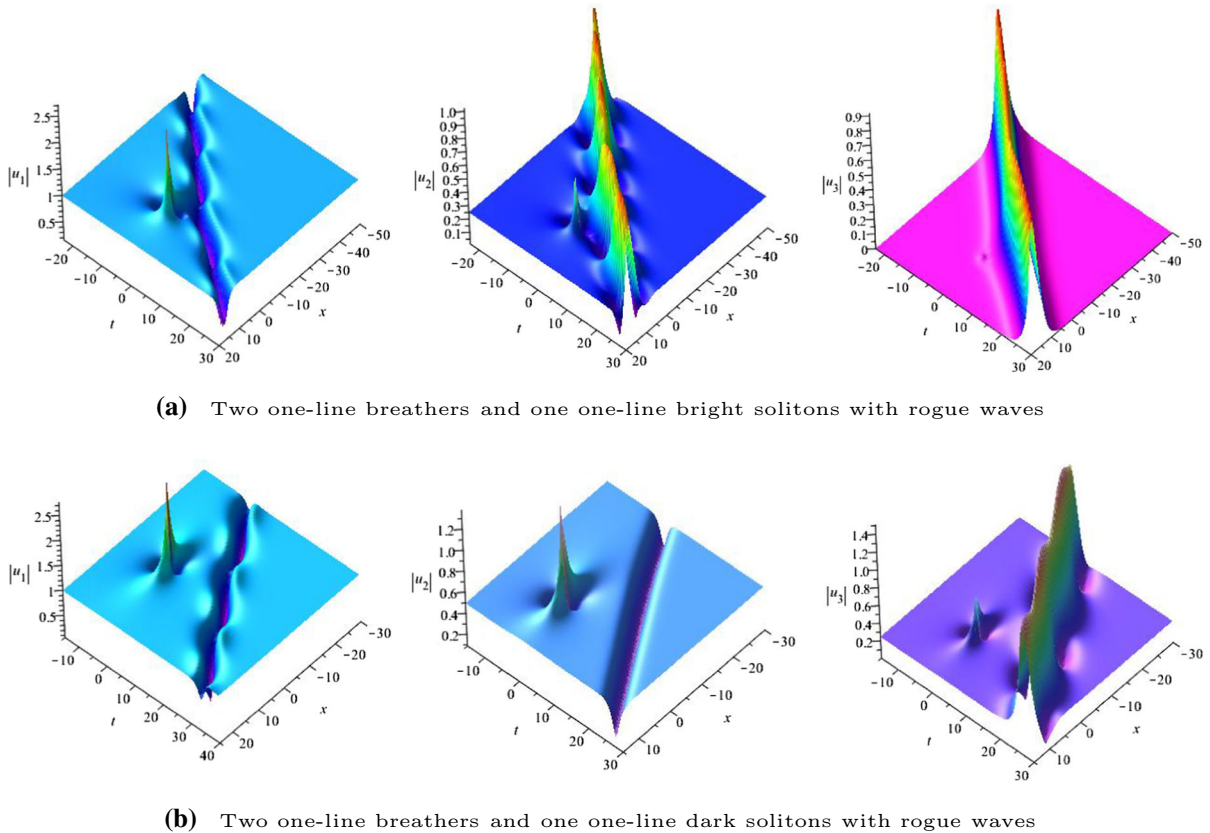


**Fig. 2** The 3-D map for case 1.2. Parameters with **a**  $a_1 = 1, a_2 = \frac{1}{4}, a_3 = 0, \alpha = \beta = 10^{-2}$  **b**  $a_1 = 1, a_2 = \frac{1}{2}, a_3 = \frac{1}{4}, \alpha = 0, \beta = 10^{-4}$  (Color online)

- (1) If the second or third background is vanished ( $a_2 = 0$  or  $a_3 = 0$ ), one component is a two-line bright soliton with second-order rogue wave and the other two components are all two-line breathers with second-order rogue waves. Here we exhibit the plot of the case  $a_3 = 0$  in Fig. 6a, the third component  $u_3$  is two-line bright soliton with a weak second-order rogue-like wave. And if  $a_2 = 0$  and other parameters are nonzero, we can also get that the second component  $u_2$  is two-line bright soliton with second-order rogue wave.
- (2) If  $\alpha = 0$  or  $\beta = 0, a_k \neq 0$ , one component is a two-line dark soliton with second-order rogue wave and the others are two-line breathers with second-order rogue waves. In Fig. 6b, when  $\alpha = 0$ , the second component  $u_2$  is two-line dark soliton with second-order rogue wave. When  $\beta = 0$ , we can also get the case that the third component  $u_3$  is two-line dark soliton with second-order rogue wave.

**Case 2.3. Breathers with second-order rogue waves.**

If all the parameters are nonzero, the three components are all two parallel breathers with second-order rogue waves in Fig. 7, which is parallel to the corresponding case of the first-order solutions. Increasing the values of  $\alpha$  or  $\beta$ , the locations of second-order rogue waves will be closer to the propagating breathers.

The higher-order semi-rational solutions also behave as three kinds of hybrid forms: (1) One component is  $N$ -line bright soliton with  $N$ -order rogue wave, the others are dark solitons with rogue waves. Alternatively, one component is  $N$ -line dark soliton with rogue wave and two are  $N$ -line bright solitons with rogue waves. (2) One component is  $N$ -line bright or dark soliton with  $N$ -order rogue wave, the others are breathers with  $N$ -order rogue waves. (3) Three components are all  $N$ -line breathers with  $N$ -order rogue waves. These conclusions are also suitable for the multiple-component FL systems. Take particular solutions similar to the

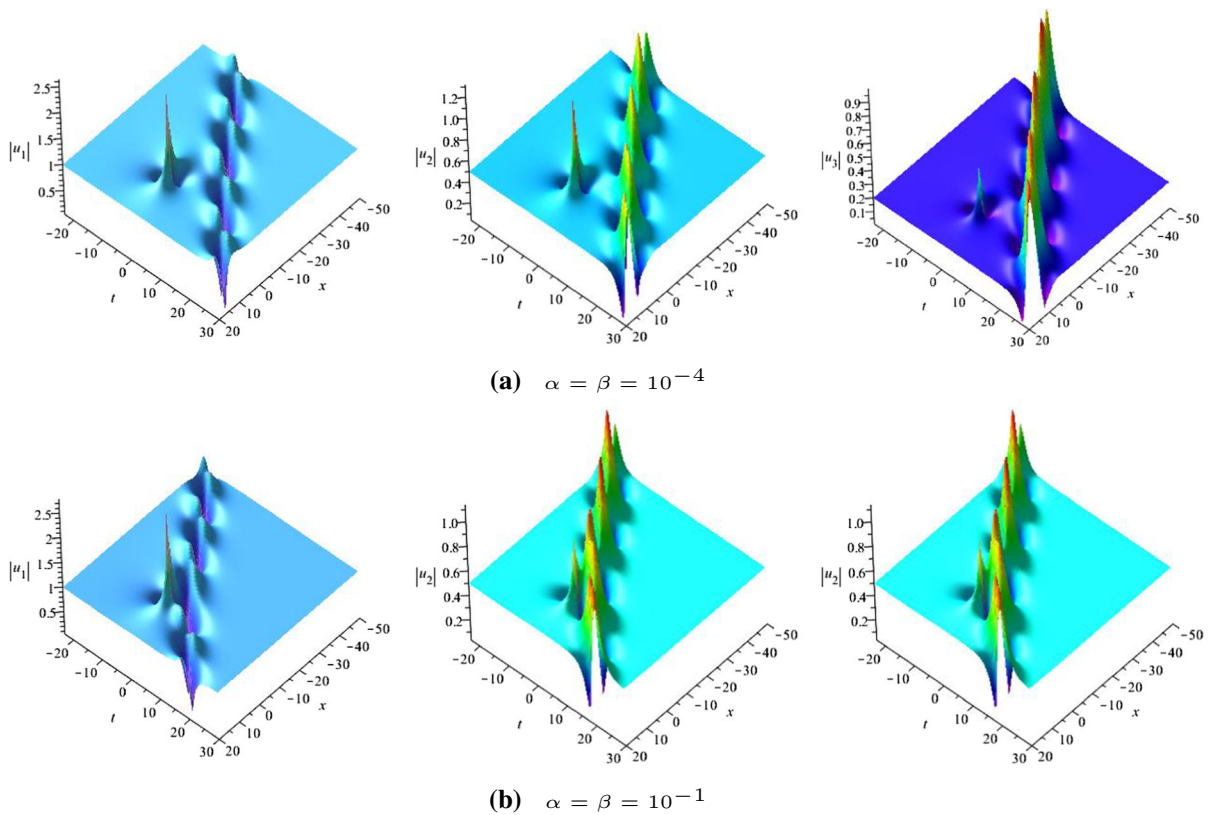


**Fig. 3** The 3-D map for case 1.3. Parameters with  $a_1 = 1, a_2 = \frac{1}{2}, a_3 = \frac{1}{5}$  (Color online)

solutions (9). Sign the altitude of the  $M$ -component background wave as  $a_k$  ( $k = 1, 2, \dots, M$ ) and the disturbing parameter in  $u_l$  as  $b_l$  for  $l = 2, 3, \dots, M - 1$ . Then the higher-order rogue waves can be obtained easily by taking  $b_l = 0$ . Besides, the following three kinds of interacting solutions can be made. If  $a_k$  and  $b_l$  are all nonzero, components  $u_1, u_2, \dots, u_M$  are all breathers with rogue waves and the features of the first component  $u_1$  is quite discrepant from the other  $M - 1$  components. Secondly, when one of the background wave except the first one is vanished ( $a_l = 0$ ), the corresponding component  $u_l$  is a bright soliton with rogue wave and the others the breathers with rogue waves. Besides, when one of the parameters  $b_l = 0$ , the corresponding component  $u_l$  performs as a dark soliton with rogue wave and others the breathers with rogue waves. Thirdly, when the first background wave ( $a_1 = 0$ ) is a zero-plane, the first component  $u_1$  is bright soliton with rogue wave and the other components are all dark solitons with rogue waves. Besides, when the value of the

parameters  $b_l$  increase, the locations of the rogue waves will be closer to the propagating solitons or breathers.

#### 4 Modulation instability of continuous waves

The modulation instability (MI) analysis is an efficient way to get the conditions for rogue waves. In this section, we analyze the MI by starting with the following steady-state ansatz as the carrier waves.

$$u_k = a_k e^{b_k x + c_k t}, \quad k = 1, 2, 3, \tag{13}$$

where  $a_k$  represents the real amplitude of the plane wave  $u_k$ ,  $b_k$  is a real wave number and  $c_k$  is the real frequency of the carrier waves for  $k = 1, 2, 3$ . Substitute (13) into system (1), then the nonlinear dispersion relations can be obtained as

$$\begin{aligned} & -a_1 c_1 b_1 - \frac{\sigma}{2} a_1 a_2^2 b_1 - \frac{1}{2} \sigma a_1 a_3^2 b_1 - a_1^3 b_1 \\ & - \frac{1}{2} a_1 \sigma a_2^2 b_2 - \frac{\sigma}{2} a_1 a_3^2 b_3 + a_1 = 0, \end{aligned}$$

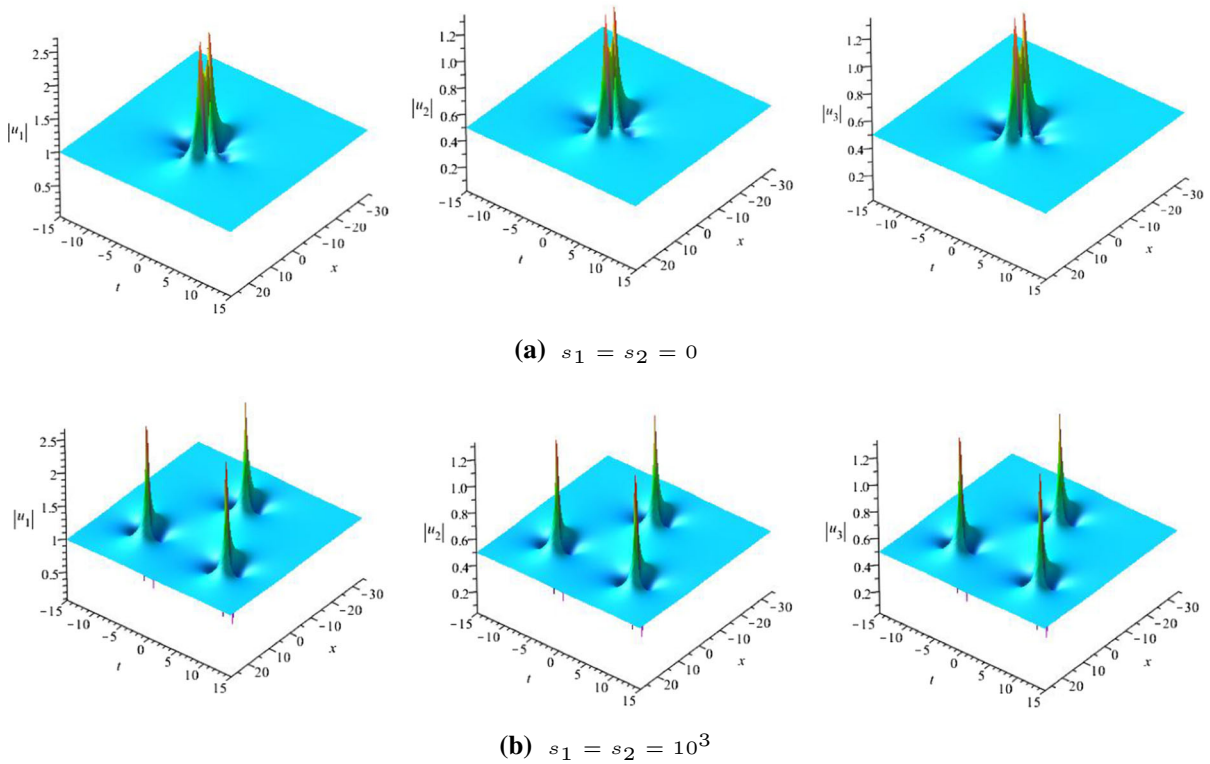


**Fig. 4** Plots of second-order rogue waves. Other parameters with  $a_1 = 1, a_2 = -\frac{1}{2}, a_3 = \frac{1}{2}, \alpha = \beta = 0$  (Color online)

$$\begin{aligned}
 & -a_2c_2b_2 - \sigma a_2^3b_2 - \frac{\sigma}{2} a_2a_3^2b_2 - \frac{1}{2} a_1^2a_2b_2 \\
 & - \frac{\sigma_2}{2} a_2 a_3^2b_3 - \frac{1}{2} a_2a_1^2b_1 + a_2 = 0, \\
 & -a_3c_3b_3 - \frac{\sigma}{2} a_2^2a_3b_3 - \sigma a_3^3b_3 - \frac{1}{2} a_1^2a_3b_3 \\
 & - \frac{\sigma}{2} a_3 a_2^2b_2 - \frac{1}{2} a_3a_1^2b_1 + a_3 = 0. \tag{14}
 \end{aligned}$$

Introducing the linear stability for the perturbed system (1)

$$u_k = (1 + \epsilon p_k) a_k e^{b_k x + c_k t}, \quad k = 1, 2, 3, \tag{15}$$

where  $\epsilon p_k$  is a small perturbation of each carrier wave. After substituting Eq. (15) into system (1), keep the linear terms only in  $\epsilon p_k$ , then we get the following equations

$$\begin{aligned}
 & 2 p_{1,x} b_1 + (-i a_2^2 b_2 - i a_3^2 b_3 + 2i) p_{1,x} \\
 & + 2i b_1 p_{1,t} + i a_1 b_1 (p_{2,x} a_2 + p_{3,x} a_3)
 \end{aligned}$$

$$\begin{aligned}
 & + (-2 a_2 (b_1 + b_2) p_2 - 2 a_3 (b_1 + b_3) p_3 \\
 & - 4 p_1 a_1 b_1) a_1 b_1 = 0, \\
 & 2 p_{2,x} b_2 + (-i a_1^2 b_1 - i a_3^2 b_3 + 2i) p_{2,x} \\
 & + 2i b_2 p_{2,t} + i a_2 b_2 (p_{1,x} a_1 + p_{3,x} a_3) \\
 & + (-2 a_1 (b_1 + b_2) p_1 - 2 a_3 (b_2 + b_3) p_3 \\
 & - 4 p_2 a_2 b_2) a_2 b_2 = 0, \\
 & 2 p_{3,x} b_3 + (-i a_1^2 b_1 - i a_2^2 b_2 + 2i) p_{3,x} \\
 & + 2i b_3 p_{3,t} + i a_3 b_3 (p_{1,x} a_1 + p_{2,x} a_2) \\
 & + [-2 (2 p_3 a_3 b_3 + a_1 (b_1 + b_3) p_1 \\
 & + a_2 (b_2 + b_3) p_2)] a_3 b_3 = 0. \tag{16}
 \end{aligned}$$

Assume that  $p_k = v_k[1]e^{i\omega(kx+t)} + v_k[2]e^{-i\omega(kx+t)}$  with  $v_k[j]$  is the complex amplitudes of the perturbation wave for  $k = 1, 2, 3, \omega$  is the MI gain. Then system (16) changes into a system of  $v_k[j]$  for  $j = 1, 2, k = 1, 2, 3$ . Since  $v_k[j]$  is not zero, the following condition can be derived.

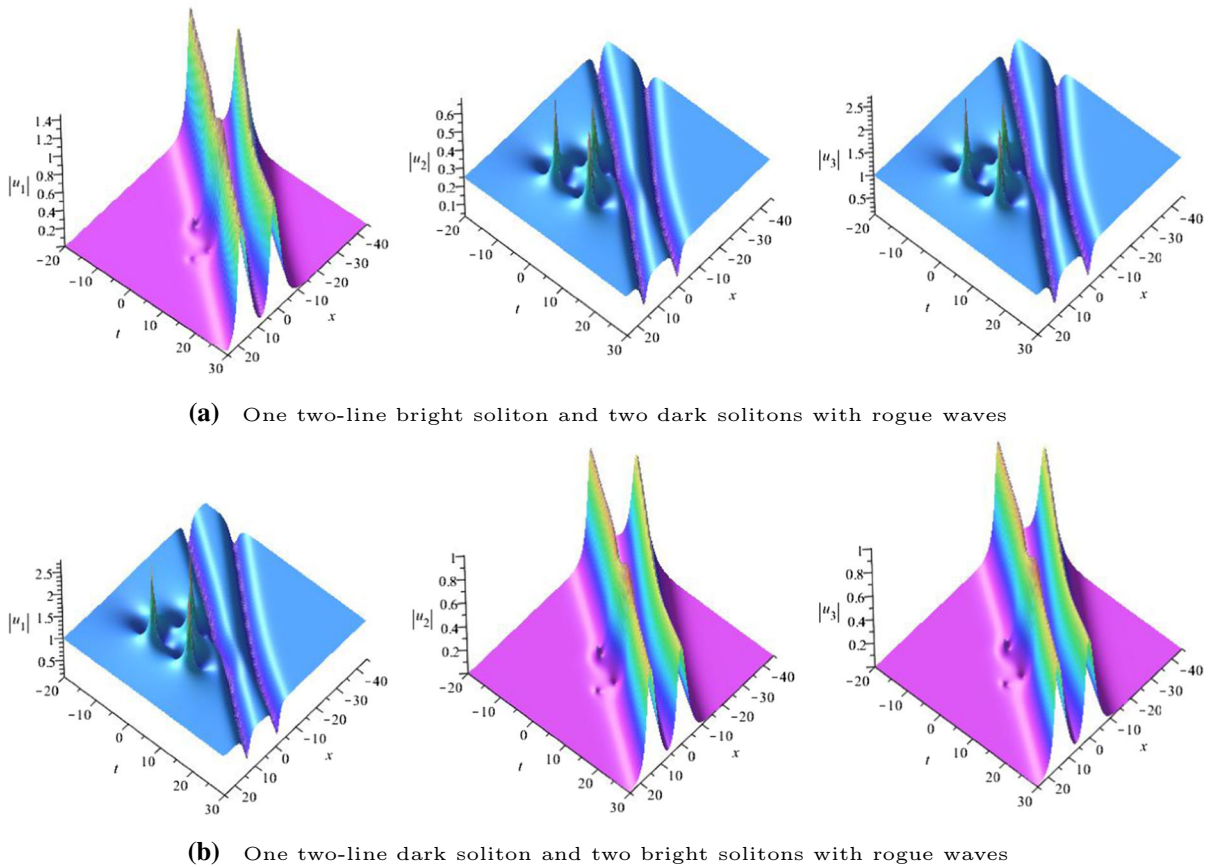
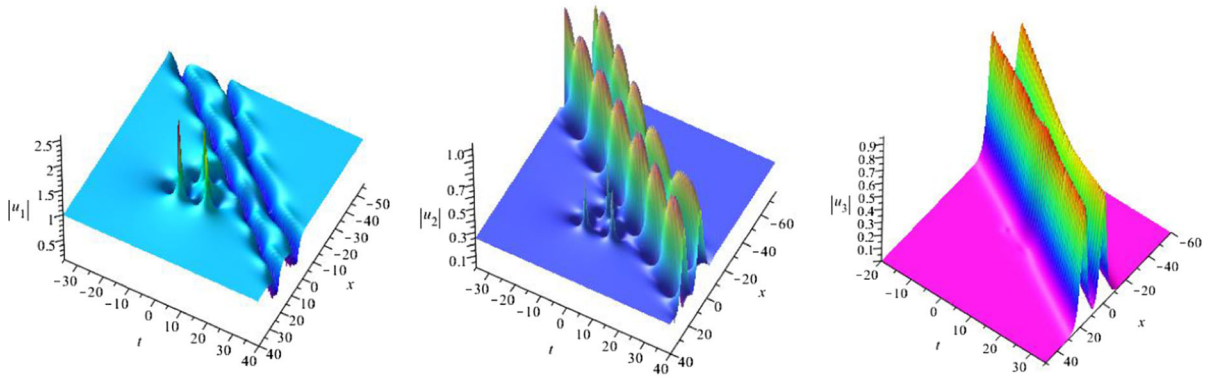


**Fig. 5** The 3-D map for case 2.1. Parameters with **a**  $a_1 = 0, a_2 = \frac{1}{4}, a_3 = 1, \alpha = \beta = 2 \times 10^{-3}, s_1 = 100, s_2 = -100$ . **b**  $a_1 = 1, a_2 = 0, a_3 = 0, \alpha = \beta = 2 \times 10^{-3}, s_1 = 100, s_2 = -100$  (Color online)

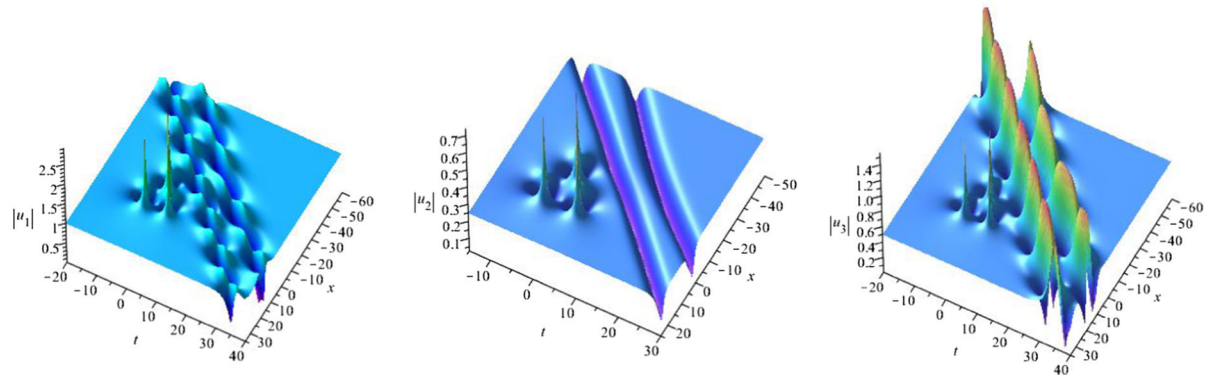
$$A = \begin{pmatrix} -a_2 r_1 a_1 & -2a_1 a_2 & A_{13} & -2\sigma a_2^2 & -a_2 r_1 \sigma a_3 & 0 \\ -r_2 a_1 a_3 & -2a_1 a_3 & -\sigma a_2 r_1 a_3 & -2\sigma a_2 a_3 & A_{25} & 0 \\ -2a_1 a_3 & r_2 a_1 a_3 & -2\sigma a_2 a_3 & \sigma a_2 r_2 a_3 & -2\sigma a_3^2 & A_{36} \\ -2a_1 a_2 & a_2 r_2 a_1 & -2\sigma a_2^2 & A_{44} & -2\sigma a_2 a_3 & \sigma a_2 a_3 (r_2 - 2) \\ -2a_1^2 & A_{52} & -2\sigma a_1 a_2 & \sigma a_2 r_2 a_1 & -2\sigma a_1 a_3 & \sigma a_1 a_3 (r_2 - 2) \\ A_{61} & -2a_1^2 & -\sigma a_2 r_1 a_1 & -2\sigma a_1 a_2 & -\sigma r_1 a_1 a_3 & 0 \end{pmatrix} = 0 \tag{17}$$

with

$$\begin{aligned} \tau &= \sigma a_2^2 + \sigma a_3^2 + a_1^2, \\ r_1 &= k\omega\tau + 2, \quad r_2 = k\omega\tau - 2, \\ A_{61} &= -2k\tau\omega^2 + (-k\tau a_1^2 - k\tau^2 - 2)\omega - 2a_1^2 \\ A_{52} &= -2k\tau\omega^2 + (k\tau a_1^2 + k\tau^2 + 2)\omega - 2a_1^2, \\ A_{13} &= -2k\tau\omega^2 + (-k\sigma\tau a_2^2 - k\tau^2 - 2)\omega - 2\sigma a_2^2, \\ A_{44} &= -2k\tau\omega^2 + (k\sigma\tau a_2^2 + k\tau^2 + 2)\omega - 2\sigma a_2^2, \\ A_{25} &= -2k\tau\omega^2 + (-k\sigma\tau a_3^2 - k\tau^2 - 2)\omega - 2\sigma a_3^2, \end{aligned}$$



(a) Two two-line breathers and one two-line bright soliton with rogue waves



(b) Two two-line breathers and one two-line dark soliton with rogue waves

**Fig. 6** The 3-D map for case 2.2. Parameters with **a**  $a_1 = 1, a_2 = \frac{1}{4}, a_3 = 0, \alpha = \beta = 2 \times 10^{-4}, s_1 = 100, s_2 = -100$ . **b**  $a_1 = 1, a_2 = \frac{1}{4}, a_3 = \frac{1}{2}, \alpha = 0, \beta = 2 \times 10^{-4}, s_1 = 100, s_1 = -100$  (Color online)

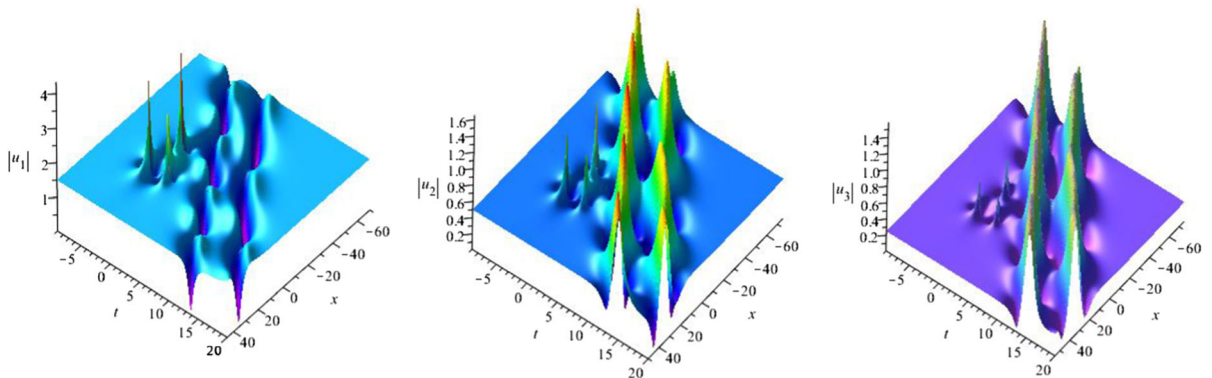


**Fig. 7** The 3-D map for case 2.3. Parameters with  $a_1 = \frac{3}{2}, a_2 = \frac{1}{2}, a_3 = \frac{1}{4}, \alpha = \beta = 10^{-4}, s_1 = 100, s_2 = -100$  (Color online)

$$A_{36} = -2k\tau\omega^2 + (k\sigma\tau a_3^2 + k\tau^2 + 2)\omega - 4\sigma a_3^2.$$

Since  $A = 0$  is a sixth-order equation of  $\omega$ , we can derive the relation

$$\begin{aligned} & (-\omega^4\tau^2 + \omega^2\tau^4)k^2 \\ & + \left[ \tau^2 - \left( (a_2^2 + 2a_3^2)\sigma + a_1^2 \right) \tau \right] \omega^2 \\ & - \omega\sigma\tau^2 a_3^2 \Big] k \\ & - a_3^2\sigma\omega - 2a_3^2\sigma\tau + \omega^2 = 0, \end{aligned} \quad (18)$$

then

$$k = \frac{\sqrt{g} + [-\tau + (a_2^2 + 2a_3^2)\sigma + a_1^2]\omega + a_3^2\sigma\tau}{-2\omega^3\tau + 2\omega\tau^3}, \quad (19)$$

with

$$\begin{aligned} g = & 4\omega^4 - 4\omega^3\sigma a_3^2 \\ & + \left[ (a_2^2 + 2a_3^2)^2\sigma^2 + \left( (4a_1^2 - 12\tau) a_3^2 \right. \right. \\ & \left. \left. - 2a_2^2(-a_1^2 + \tau) \right) \sigma \right] \omega^2 \\ & + (a_1^4 - 2\tau a_1^2 - 3\tau^2)\omega^2 + 2 \left[ (a_2^2 + 2a_3^2)\sigma \right. \\ & \left. + a_1^2 + \tau \right] a_3^2\tau\sigma\omega + \sigma^2\tau^2 a_3^4 + 8\sigma\tau^3 a_3^2. \end{aligned}$$

When  $g > 0$ ,  $\text{Im}(k) = 0$ ,  $k$  is real and the plane wave background is stable under the perturbations  $p_k$ . But when  $g < 0$ ,  $\text{Im}(k) \neq 0$ .  $k$  is complex, the small perturbations grow exponentially with  $x$ , the MI occurs.

## 5 Conclusion

In summary, we generalize the three-component coupled FL system and the corresponding Lax pair are derived. Then the generalized  $(n, M)$ -fold DT is constructed. Compared to the semi-rational solutions of the two-component coupled FL system in [13], for the number of the component increase, the solutions of the three-component system have more abundant structures. In case 1.2 and case 2.2, we also get the mixed localized solutions that one component is a bright or dark soliton with rogue wave and the other two are breathers with rogue waves. But for the two-component system in [13], these kinds of solutions have not been found. Moreover, in this paper, the higher-order mixed localized solutions also present as the higher-order

rogue waves, respectively, emerging in three kinds of arrangements: (1) One component is  $N$ -line bright soliton, and the others are  $N$ -line dark solitons. Alternatively, one component is  $N$ -line dark soliton and the other two are  $N$ -line bright solitons. (2) One component is  $N$ -line bright or dark soliton, and the others are  $N$ -line breathers. (3) Three components are all  $N$  parallel breathers. These results can also be generalized to the  $N$ -component FL system. Besides, the modulation instability conditions of the plane-wave solutions for system (1) are present.

However, some significant limitations need to be considered. Firstly, for the second-order mixed localized solutions, we have not obtained the solution that rogue waves emerging in the spread of the coexistence wave of the breather and line soliton. Secondly, the expressions of second-order or even higher-order solutions are cumbersome; we cannot show them in concise forms. Furthermore, the solutions in determinant forms would be of great help in the analysis of the components.

These findings enhance our understandings of the localized solution structures for the multi-component FL system. We hope these results will be matched with the physical experiments later.

**Acknowledgements** The first author would like to express her sincere thanks to Xu Tao for his valuable comments. The authors gratefully acknowledge the support of National Natural Science Foundation of China (Nos. 11675054, 11435005) and Science and Technology Commission of Shanghai Municipality (No. 18dz2271000).

## Compliance with ethical standards

**Conflict of interest** The authors declare that there is no conflict of interests regarding the publication of this paper.

## References

1. Fokas, A.S.: On a class of physically important integrable equations. *Physica D* **87**, 145–150 (1995)
2. Lenells, J., Fokas, A.S.: On a novel integrable generalization of the nonlinear Schrödinger equation. *Nonlinearity* **22**, 11–27 (2008)
3. Triki, H., Wazwaz, A.M.: Combined optical solitary waves of the Fokas–Lenells equation. *Wave Random Complex* **27**, 587–593 (2017)
4. Matsuno, Y.: A direct method of solution for the Fokas–Lenells derivative nonlinear Schrödinger equation: II. Dark soliton solutions. *J. Phys. A Math. Theor.* **45**, 475202 (2012)

5. Xu, J., Fan, G.: Long-time asymptotics for the Fokas–Lenells equation with decaying initial value problem: without solitons. *J. Differ. Equ.* **259**, 1098–1148 (2015)
6. Triki, H., Wazwaz, A.M.: New types of chirped soliton solutions for the Fokas–Lenells equation. *Int. J. Numer. Method Heat* **27**, 00–00 (2017)
7. Xu, S.W., He, J.S., Cheng, Y., Porseizan, K.: The  $n$ -order rogue waves of Fokas–Lenells equation. *Math. Method Appl. Sci.* **38**, 1106–1126 (2015)
8. Zhang, Y., Yang, J.W., Chow, K.W., Wu, F.: Solitons, breathers and rogue waves for the coupled Fokas–Lenells system via Darboux transformation. *Nonlinear Anal. Real* **33**, 237–252 (2017)
9. Ahmed, I., Seadawy, A.R., Lu, D.C.: M-shaped rational solitons and their interaction with kink waves in the Fokas–Lenells equation. *Phys. Scr.* **94**, 5:055205 (2019)
10. Kundu, A.: Two-fold integrable hierarchy of nonholonomic deformation of the derivative nonlinear Schrödinger and the Lenells–Fokas equation. *J. Math. Phys.* **51**, 022901 (2010)
11. Ling, L.M., Feng, B.F., Zhu, Z.N.: General soliton solutions to a coupled Fokas–Lenells equation. *Nonlinear Anal. Real* **40**, 185–214 (2018)
12. Wang, X., Wei, J., Wang, L.: Baseband modulation instability, rogue waves and state transitions in a deformed Fokas–Lenells equation. *Nonlinear Dyn.* **97**, 343–353 (2019)
13. Xu, T., Chen, Y.: Semirational solutions to the coupled Fokas–Lenells equations. *Nonlinear Dyn.* **45**, 918–941 (2019)
14. Lambert, F., Willox, R.: On the balance between dispersion and nonlinearity for a class of bilinear equations. *J. Phys. Soc. Jpn.* **58**, 1860–1861 (2007)
15. Solli, D.R., Ropers, C., Koonath, P., Jalali, B.: Optical rogue waves. *Nature* **450**, 1054–1058 (2007)
16. Ablowitz, M.J., Horikis, T.P.: Interacting nonlinear wave envelopes and rogue wave formation in deep water. *Phys. Fluids* **27**, 012107 (2015)
17. Akhmediev, N.N., Korneev, V.I.: Modulation instability and periodic solutions of the nonlinear Schrödinger equation. *Theor. Math. Phys.* **69**, 1089–1093 (1986)
18. Akhmediev, N., Soto-Crespo, J.M., Ankiewicz, A.: Extreme waves that appear from nowhere: on the nature of rogue waves. *Phys. Lett. A* **373**, 2137–2145 (2009)
19. Terng, C.L., Uhlenbeck, K.: Bäcklund transformations and loop group actions. *Commun. Pure Appl. Math.* **53**, 1–75 (2000)
20. Guo, B.L., Ling, L.M., Liu, Q.P.: Nonlinear Schrödinger equation: generalized Darboux transformation and rogue wave solutions. *Phys. Rev. E* **85**, 026607 (2012)
21. Ling, L.M., Zhao, L.C., Guo, B.L.: Darboux transformation and classification of solution for mixed coupled nonlinear Schrödinger equations. *Commun. Nonlinear Sci.* **32**, 285–304 (2016)
22. Wen, X.Y., Yan, Z.Y., Yang, Y.Q.: Dynamics of higher-order rational solitons for the nonlocal nonlinear Schrödinger equation with the self-induced parity-time-symmetric potential. *Chaos* **26**, 063123 (2016)
23. Wang, X., Li, Y.Q., Chen, Y.: Generalized Darboux transformation and localized waves in coupled Hirota equations. *Wave Motion* **51**, 1149–1160 (2014)
24. Wen, X.Y., Yan, Y.: Higher-order rational solitons and rogue-like wave solutions of the  $(2 + 1)$ -dimensional nonlinear fluid mechanics equations. *Commun. Nonlinear Sci.* **43**, 311–329 (2017)
25. Abrarov, R.M., Christiansen, P.L., Darmanyan, S.A., Scott, A.C., Soerensen, M.P.: Soliton propagation in three coupled nonlinear Schrödinger equations. *Phys. Lett. A* **171**, 298–302 (1992)
26. Xia, T.C., Fan, E.G.: The multi-component generalized Kaup–Newell hierarchy and its multi-component integrable couplings system with two arbitrary functions. *J. Math. Phys.* **46**, 043510 (2005)
27. Ling, L.M., Zhao, L.C., Guo, B.L.: Darboux transformation and multi-dark soliton for  $N$ -component nonlinear Schrödinger equations. *Nonlinearity* **28**, 3243 (2015)
28. Chen, J.C., Chen, Y., Feng, B.F., Maruno, K.I.: Rational solutions to two- and one-dimensional multi-component Yajima–Oikawa systems. *Phys. Lett. A* **379**, 1510–1519 (2015)
29. Zhang, H.Q., Wang, Y., Ma, W.X.: Binary Darboux transformation for the coupled Sasa–Satsuma equations. *Chaos* **27**, 597 (2017)
30. Zhang, Z., Tian, B., Liu, L., Sun, Y., Du, Z.: Lax pair, breather-to-soliton conversions, localized and periodic waves for a coupled higher-order nonlinear Schrödinger system in a birefringent optical fiber. *Eur. Phys. J. Plus* **134**, 129 (2019)
31. Lou, S.Y.: Generalized dromion solutions of the  $(2 + 1)$ -dimensional KdV equation. *J. Phys. A Math. Theor.* **28**, 7227–7232 (1995)
32. Hirota, R.: Nonlinear partial difference equations. IV. Bäcklund transformation for the discrete-time Toda equation. *J. Phys. Soc. Jpn.* **45**, 321–332 (1978)
33. Hua, Y.F., Guo, B.L., Ma, W.X., Lv, X.: Interaction behavior associated with a generalized  $(2+1)$ -dimensional Hirota bilinear equation for nonlinear waves. *Appl. Math. Model.* **74**, 184–198 (2019)
34. Ma, W.X., Yong, X.L., Zhang, H.Q.: Diversity of interaction solutions to the  $(2 + 1)$ -dimensional Ito equation. *Comput. Math. Appl.* **75**, 289–295 (2018)
35. Yin, Y.H., Ma, W.X., Liu, J.G., Lv, X.: Diversity of exact solutions to a  $(3 + 1)$ -dimensional nonlinear evolution equation and its reduction. *Comput. Math. Appl.* **76**, 1275–1283 (2018)
36. Huang, Y.F., Guo, B.L., Ma, W.X., Lv, X.: Interaction behavior associated with a generalized  $(2 + 1)$ -dimensional Hirota bilinear equation for nonlinear waves. *Appl. Math. Lett.* **74**, 184–198 (2019)
37. Matveev, V.B., Salle, M.A.: *Darboux Transformations and Solitons*. Springer, New York (1991)
38. Gu, C.H., Hu, H.S., Zhou, Z.X.: *Darboux Transformations in Integrable Systems: Theory and Their Applications*. Springer, Berlin (2005)
39. Nimmo, J.J.C., Freeman, N.C.: The use of Bäcklund transformations in obtaining  $N$ -soliton solutions in Wronskian form. *J. Phys. Math. Gen.* **17**, 1415–1424 (1984)
40. Gao, L.N., Zi, Y.Y., Yin, Y.H., Ma, W.X., Lv, X.: Bäcklund transformation, multiple wave solutions and lump solutions to a  $(3 + 1)$ -dimensional nonlinear evolution equation. *Nonlinear Dyn.* **89**, 2233–2240 (2017)
41. Zhu, Q.Z., Xu, J., Fan, E.G.: The Riemann–Hilbert problem and long-time asymptotics for the Kundu–Eckhaus equation

- with decaying initial value. *Appl. Math. Lett.* **76**, 81–89 (2018)
42. Zhang, X.E., Chen, Y.: Inverse scattering transformation for generalized nonlinear Schrödinger equation. *Appl. Math. Lett.* **98**, 306–313 (2019)
43. Zhang, G.Q., Yan, Y.: Three-component nonlinear Schrödinger equations: modulational instability, Nth-order vector rational and semi-rational rogue waves, and dynamics. *Commun. Nonlinear Sci.* **62**, 117–133 (2018)
44. Xu, T., Chen, Y.: Mixed interactions of localized waves in the three-component coupled derivative nonlinear Schrödinger equations. *Nonlinear Dyn.* **92**, 2133–2142 (2018)
45. Wang, X., Yang, B., Chen, Y., Yang, Q.: Higher-order localized waves in coupled nonlinear Schrödinger equations. *Chin. Phys. Lett.* **31**, 090201 (2014)

**Publisher's Note** Springer Nature remains neutral with regard to jurisdictional claims in published maps and institutional affiliations.